Ecological Modelling 317 (2015) 30–40

Contents lists available at ScienceDirect

Ecological Modelling

journal homepage: www.elsevier.com/locate/ecolmodel

An experimentally validated nitrate–ammonium–phytoplankton model including effects of starvation length and ammonium inhibition on nitrate uptake

Martino E. Malerba[a,b,c,e,*], Sean R. Connolly[c,d], Kirsten Heimann[c,e]

[a] AIMS@JCU, James Cook University, Townsville, QLD, Australia
[b] Australian Institute of Marine Science, Townsville, QLD, Australia
[c] College of Marine and Environmental Sciences, James Cook University, Townsville, QLD, Australia
[d] Australian Research Council Centre of Excellence for Coral Reef Studies, James Cook University, Townsville, QLD, Australia
[e] Centre for Sustainable Tropical Fisheries and Aquaculture, Townsville, QLD, Australia

ARTICLE INFO

Article history:
Received 15 May 2015
Received in revised form 19 August 2015
Accepted 21 August 2015

Keywords:
Phytoplankton dynamics
Quota model
Nitrogen limitation
Nitrate starvation
Ammonium inhibition
Chlorophyta

ABSTRACT

Nitrate and ammonium are the two most important ionic forms of inorganic nitrogen driving biomass production in marine and freshwater aquatic systems. The performance of plants and algae often changes when reared with either of these two forms of nitrogen individually, as well as when they are both present, or when cells have experienced previous periods of nitrogen starvation. Current functional responses quantifying how ambient nitrogen drives changes in population density are unable to capture interacting and transient effects of nitrate and ammonium. Hence, in this paper we formulate, calibrate, and test a new nitrate–ammonium quota model that accounts for nitrate and ammonium uptake, as well as the effects of nitrogen starvation length and ammonium-induced nitrate uptake inhibition. We fit the model with several time-series from the green alga *Chlorella* sp. reared in laboratory batch cultures under multiple initial conditions. We show that a single set of calibrated model parameters can capture time-series collected from experiments inoculated at 12 different initial concentrations of nitrate, ammonium, and biomass. The model also performed well when validated against time-series from two novel initial conditions withheld from model calibration. Our model therefore provides a framework for evaluating the potential broader ecological and environmental consequences of ambient nitrate and ammonium regimes for phytoplankton communities in nature and aquaculture.

1. Introduction

All living organisms require nitrogen (N) for the production of new biomass. While heterotrophic organisms rely exclusively on organic N from their diet, autotrophic organisms can also absorb inorganic N from the environment (Crawford et al., 2000). Ammonium and nitrate are the two most common ionic (reactive) forms of inorganic N, and their assimilation by plants and photosynthetic algae quantitatively dominates the nitrogen cycle (Gruber, 2008; Zehr and Ward, 2002). However, the way autotrophic organisms incorporate these two N differs. Ammonium is easier to assimilate because most amino acids are in the same oxidation state; in contrast, nitrate must be first reduced to ammonium by means of specialized enzymes and then assimilated (Berges, 1997; Guerrero et al., 1981; Syrett, 1981). This key difference between nitrate and ammonium assimilation leads to different assimilation kinetics in autotrophic organisms, which have far reaching implications in many areas, including understanding changes in species competition (Donald et al., 2011; Jackson et al., 1989), evaluating the effects of eutrophication (Cox et al., 2009), quantifying fluxes of the nitrogen cycle (Fowler et al., 2013), and analyzing optimal fertilization for industrial production (Michalczyk et al., 2014).

Assimilation of nitrate and ammonium is particularly important for phytoplankton, estimated to be responsible for around 30–40% of global primary productivity (Duarte and Cebrià n, 1996). Nitrate and ammonium concentrations in natural environments affect phytoplankton ecology, by selecting for different phytoplankton species (Donald et al., 2011) or modifying the risk for algal bloom formation (Dugdale et al., 2007). Because of the importance of N sources in phytoplankton ecology, numerous studies over the last 40 years have documented a range of processes

* Corresponding author at: James Cook University, College of Marine and Environmental Sciences, Townsville, 4811 QLD, Australia. Tel.: +61 7 4781 3174.
E-mail address: Martino.Malerba@my.jcu.edu.au (M.E. Malerba).

http://dx.doi.org/10.1016/j.ecolmodel.2015.08.024
0304-3800/

regulating nitrate–ammonium assimilation kinetics in phytoplankton cells (Dortch, 1990; Flynn et al., 1997). First, phytoplankton cells can display different degrees of specialization toward ammonium or nitrate by presenting better kinetic parameters when reared with either source of N (here referred to as "preference"; reviewed in Dortch, 1990). Second, supplying ammonium can repress the nitrate uptake of a cell by either altering the activity of specific transport enzymes or by preventing their synthesis (Berges, 1997; L'Helguen et al., 2008; "inhibition"; Morris and Syrett, 1963; although not all species are affected, Mulholland and Lomas, 2008). Physiological studies have determined that the observed ammonium-induced inhibition is a product of the ammonium assimilation pathway, which often impairs the ability of a cell to assimilate nitrate (Rigano et al., 1979; Syrett and Morris, 1963). Third, periods of N starvation can lead to an initial delay in nitrate assimilation and cell division ("starvation"; De La Rocha et al., 2010; Dortch et al., 1982; Martinez, 1991). However, our understanding of these phenomena is incomplete; in particular, we do not know how processes of preference, starvation and inhibition can interact to simultaneously influence phytoplankton dynamics under different nitrate and ammonium concentrations. This aspect can be important in multiple fields. In nature, phytoplankton communities can be exposed to periods of N starvation with episodic and cyclic resupplies of nitrate or ammonium (Priddle et al., 1997; Young and Beardall, 2003). In aquaculture, imposing periods of N limitation can increase the quality of the final product by increasing the specific lipid content in the biomass (Griffiths et al., 2014). Finally, managing aquatic environments also involve regulating nitrate-polluting (e.g. land clearing, agriculture) and ammonium-polluting activities (e.g. human waste discharge, intensive livestock) in order to minimize risks of algal bloom formation (Domingues et al., 2011).

Some time ago, Dortch (1990) called for an improved approach for quantifying N utilization in single species to make better sense of phytoplankton dynamics in nature. Molecular methods of measuring the activity of assimilatory enzymes can provide important information about N utilization (Fan et al., 2003; Lomas, 2004), but quantifying N uptake and its conversion into producer biomass still requires monitoring total phytoplankton assimilation (either directly with isotope techniques, or indirectly from ambient N depletion) and producer population densities (Bronk et al., 2007). Typically, species-specific kinetic estimates for per-cell N uptake are calculated by dividing N consumed by cell density at successive points in time, and then fitting a saturating Michaelis–Menten functional response (Laws et al., 2011; Maguer et al., 2007; Tantanasarit et al., 2013). While convenient when analyzing rates of N utilization under constant nutrient regimes, this technique cannot tractably capture the functional relationships that govern important processes, such as interactions between nitrate and ammonium uptake and acclimatization following extended starvation periods. Furthermore, the precision of this technique is limited by the fact that each estimate for per capita uptake rate is based on only two observations at successive times. One way forward is to develop a more process-oriented framework for modeling nitrate and ammonium utilization in phytoplankton also accounting for the interactive and transient dynamics involved in this process.

In this study, we develop, calibrate, and test a model to characterize nitrate–ammonium utilization of phytoplankton populations reared in laboratory conditions, including transient effects of preference, starvation, and inhibition. The only previous models describing nitrate–ammonium utilization in phytoplankton cells (without the effect of starvation) are very detailed, explicitly characterizing the main biochemical processes that regulate the flows between multiple internal pools of different N forms (Flynn and Fasham, 1997; Flynn et al., 1997). Such a modeling approach requires estimates of biochemical rate parameters that can only be obtained from expensive and time-consuming measurements that are very rarely made in N utilization experiments. For example, the ANIM model of Flynn et al. (1997) requires estimates of the shape parameters for the size of the glutamine pool that stops NH_4 uptake (*NH4mGLN*), for the maximum size of the nitrate and ammonium internal pools assuming a maximum biomass N:C ratio (*NO3Pm*, *NH4Pm*), and for the curve characterizing glutamine suppression of nitrate–nitrite reductase synthesis (*NNiRhGLN*). Indeed, as yet, no comprehensive set of parameter estimates for any such model has been obtained for any species. Our goal here is to sacrifice the explicit characterization of the dynamics of multiple intracellular N pools, and instead to construct more tractable models whose best-fit parameter values and 95% confidence limits can be estimated from time-series of external nutrient concentrations and population size, variables that are commonly measured in phytoplankton laboratory cultures. Our results show that transient and interactive processes between nitrate and ammonium uptake play an important role determining the dynamics of our species. The present approach contributes to a more comprehensive understanding of the factors underpinning the high variation in nitrate–ammonium assimilation observed in natural and experimental systems.

2. Methods

2.1. Model

To analyze nitrate–ammonium utilization in *Chlorella* sp., we first design a process-based model derived from our current understanding of the biological processes acting on the study system (see Table 1 for parameter definitions and units). Our model extends the commonly used "Quota" model for a single nitrogen (N) source (Droop, 1975; Legovic and Cruzado, 1997), to explicitly account for two different N sources (i.e. nitrate and ammonium) and how they drive cell division. In the original Quota model, cells are assumed to assimilate a single generic N form and divide at a rate that is proportional to their internal N concentration as follows:

$$\frac{dN}{dt} = -f_N(N(t)) \times B(t) \tag{1a}$$

$$\frac{dQ}{dt} = f_N(N(t)) - \mu_{max} \times \left(1 - \frac{Q_{min}}{Q(t)}\right) \times Q(t) \tag{1b}$$

$$\frac{dB}{dt} = \mu_{max} \times \left(1 - \frac{Q_{min}}{Q(t)}\right) \times B(t) \tag{1c}$$

where $N(t)$, $Q(t)$, and $B(t)$ represent external N, internal N within each cell, and population density, respectively, as a function of time, $f_N(N(t))$ represents the functional response quantifying uptake rate as a function of medium N concentration, μ_{max} is the growth rate of a cell at infinite internal N, and Q_{min} is the threshold of internal N concentration at which no cell division occurs.Our formulation extends this framework by allowing N to be assimilated as either nitrate or ammonium. In doing so, we account for the main interactions known to regulate nitrate and ammonium utilization in phytoplankton cells (Dortch, 1990).

We use two saturating functional responses for each N type:

$$f_{NO_3}(NO_3(t), NH_4(t)) = \nu_{NO_3} \times \frac{NO_3(t)}{NO_3(t) + k_{NO_3}} \times I_{sNO_3}\left(r_{NO_3}, t\right) \times I_{inh}(NH_4(t)) \tag{2a}$$

$$f_{NH_4}(NH_4(t)) = \nu_{NH_4} \times \frac{NH_4(t)}{NH_4(t) + k_{NH_4}} \tag{2b}$$

where ν_{NO_3} and ν_{NH_4} represent the maximum feasible per-cell uptake rate, and k_{NO_3} and k_{NH_4} specify the half-saturation constants, for nitrate and ammonium, respectively. $I_{sNO_3}\left(r_{NO_3}, t\right)$ and $I_{inh}(NH_4(t))$ are indicator functions (i.e.

Table 1
Summary table of model state variables and parameters. Maximum likelihood estimates are reported only for those parameters in the model selected by AIC (cf. Table 2 for AIC scores). Hence, parameter best estimates for the functional response for the hyperbolic nitrogen uptake were not reported as the best-fitting model has a linear uptake. Also d_{NO_3} was not reported, as the best-fitting model does not have delayed nitrate starvation. The 95% profile likelihood intervals are shown in parentheses.

State variables	Definition (units)	
NO_3	Nitrate in medium (μmol NO_3^- L^{-1})	
NH_4	Ammonium in medium (μmol NH_4^+ L^{-1})	
Q	Nitrogen quota (μmol N $cell^{-1}$)	
B	Population density (cell L^{-1})	
Parameters	**Definition (units)**	**Mean (±95% CI)**
v_{NO_3}	Maximum per-capita nitrate uptake rate (μmol NO_3^- $cell^{-1}$ day^{-1})	–
k_{NO_3}	Nitrate half-saturation constant (μmol NO_3^- L^{-1})	–
w_{NO_3}	Rate of daily per-capita nitrate uptake ($cell^{-1}$ day^{-1})	$9.82\,(9.03–10.5)\times10^{-11}$
v_{NH_4}	Maximum per-capita ammonium uptake rate (μmol NH_4^+ $cell^{-1}$ day^{-1})	–
k_{NH_4}	Ammonium half-saturation constant (μmol NH_4^+ L^{-1})	–
w_{NH_4}	Rate of daily per-capita ammonium uptake ($cell^{-1}$ day^{-1})	$6.74\,(5.88–7.17)\times10^{-11}$
c_{NO_4}	Recovery rate of the nitrate assimilation systems following a period of nitrogen starvation ($days^{-1}$)	0.088 (0.074–0.093)
d_{NO_3}	Length of nitrogen starvation that a cell can withstand without displaying negative effects on nitrate assimilation systems (days)	–
$f_{NH_4\_crit}$	Critical ammonium uptake rate above which the nitrate uptake of a cell is repressed (μmol NH_4^+ L^{-1} day^{-1})	$1.08\,(1.02–1.21)\times10^{-8}$
Q_{min}	Per-capita minimum nitrogen quota (μmol N $cell^{-1}$)	$3.10\,(2.36–3.67)\times10^{-8}$
μ_{max}	Growth rate at infinite nutrient storage (day^{-1})	16.10 (9.02–19.1)
t_{st}	Experimental period of nitrogen starvation imposed on the culture before the experiment (days)	Fixed experimentally
r_{NO_3}	Length of starvation-induced delay before a cell can resume nitrate uptake (days)	Calculated via Eq. (3) from c_{NO_3}, d_{NO_3}, and t_{st}

functions whose values are either 0 or 1). $I_{sNO_3}(r_{NO_3}, t)$ indicates whether or not recovery from starvation has occurred and depends on the starvation status of the cell $\left(r_{NO_3}\right)$. Finally, $I_{inh}(NH_4(t))$ indicates whether ammonium-induced nitrare uptake inhibition is occurring.

Studies on nitrate assimilation have found that, when a culture is N starved, the conversion of NO_3^- into assimilated N can require some time to be reactivated. This is because non-constitutive enzymes (e.g. nitrate reductase) need an induction period after extended lack of use. Hence, upon resupply of nitrate, there can be an initial time lag required for a cell to reactivate the N assimilation pathways (Martinez, 1991). Previous studies have also found that extended starvation lengths are associated with an increasingly long period required for the culture to acclimatize to nitrate repletion (De La Rocha et al., 2010; Martinez, 1991). To reproduce this behavior, we assume that each cell can withstand a period of length d_{NO_3} without displaying starvation symptoms for nitrate. Further increases in starvation time (t_{st}) will require a proportionally longer rehabilitation period:

$$r_{NO_3} = \begin{cases} 0 & \text{if} \quad t_{st} < d_{NO_3} \\ c_{NO_3} \times \left(t_{st} - d_{NO_3}\right) & \text{otherwise} \end{cases} \tag{3}$$

where c_{NO_3} is the sensitivity of the rehabilitation period to starvation time. During the rehabilitation period cells cannot assimilate N $\left(I_{sNO_3} = 0\right)$, and they return to normal assimilation once rehabilitated $\left(I_{sNO_3} = 1\right)$, as per:

$$I_{sNO_3}\left(r_{NO_3}, t\right) = \begin{cases} 0 & \text{when} \quad t < r_{NO_3} \\ 1 & \text{otherwise} \end{cases} \tag{4}$$

Eq. (4) imposes a step-function in N uptake: it is either zero, or equal to its normal predicted uptake. We considered smoother (sigmoid) transition functions, but in practice, the transition from zero to approximately normal uptake was rapid, relative to our daily sampling interval, which meant that the step-function was adequate to characterize the response in our experiments.

Most previous models have often assumed the process of ammonium inhibition on nitrate uptake to be a function of ambient ammonium concentration. However, physiological studies have documented that is the assimilation of ammonium (not its external concentration) that inhibits the nitrate uptake of a cell. Furthermore, the form of functional response for ammonium inhibition over nitrate uptake changes depending on the species (Dortch, 1990; L'Helguen et al., 2008). In Chlorophyceae and Cyanophyceae, ammonium addition often causes an immediate cessation of nitrate utilization (Cullimore and Sims, 1981; Pistorius et al., 1978; Syrett and Morris, 1963; Thacker and Syrett, 1972). Hence, in this study nitrate uptake inhibition is assumed to follow a step-function, where the uptake of ammonium above a critical level $\left(f_{NH_4\_crit}\right)$ fully represses nitrate uptake:

$$I_{inh}(NH_4(t)) = \begin{cases} 1 & \text{if} \quad f_{NH_4}(NH_4(t)) < f_{NH_4\_crit} \\ 0 & \text{otherwise} \end{cases} \tag{5}$$

However, alternative functional responses representing a linear or an exponentially decreasing inhibition may be more suitable for diatoms (Parker, 1993), coccolithophores (Varela and Harrison, 1999) or dinoflagellate species (Collos et al., 2004), and could readily be accommodated within the modeling framework presented here.

The full structure of our nitrate–ammonium model for batch cultures is:

$$\frac{dNO_3}{dt} = -f_{NO_3}(NO_3(t), NH_4(t)) \times B(t) \tag{6a}$$

$$\frac{dNH_4}{dt} = -f_{NH_4}(NH_4(t)) \times B(t) \tag{6b}$$

$$\frac{dQ}{dt} = \left[f_{NO_3}(NO_3(t), NH_4(t)) + f_{NH_4}(NH_4(t))\right] - \mu_{max} \times \left(1 - \frac{Q_{min}}{Q(t)}\right) \times Q(t) \tag{6c}$$

$$\frac{dB}{dt} = \mu_{max} \times \left(1 - \frac{Q_{min}}{Q(t)}\right) \times B(t) \tag{6d}$$

where $f_{NO_3}(NO_3(t), NH_4(t))$ and $f_{NH_4}(NH_4(t))$ are specified by Eqs. (2a,b)–(5) (see Fig. 1 for conceptual diagram and Table 1 for a summary table of model parameters). In this model, assimilated nitrate and ammonium are jointly stored in an internal N quota

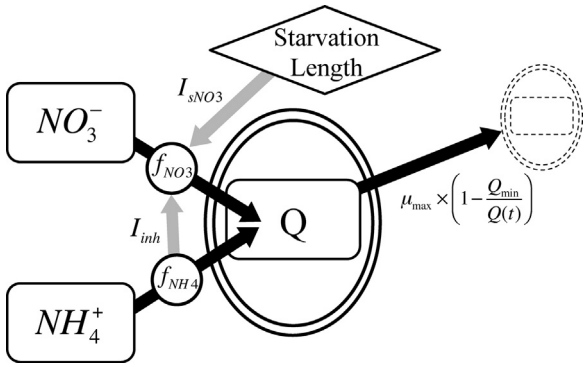

Fig. 1. Model diagram for nitrate (NO_3^-) and ammonium (NH_4^+) utilization in phytoplankton cells. The double-lined ellipse represents the cell wall of a single cell. Squares indicate the state variables for the different forms of nitrogen, either in the medium or inside the cell. The diamond represents the starvation length. Black arrows describe nitrogen flows in the system. Gray arrows indicate inhibitor mechanisms on the per-cell nitrate uptake rate. Nitrate and ammonium are taken up through the membrane and stored inside the cell. The production of new cells (dashed lines) is a saturating function of internal nitrogen concentration (Q), whose shape is determined by the parameters for maximum growth rate (μ_{max}) and minimum internal nitrogen (Q_{min}). See Table 1 and Eqs. (1a–c)–(6a–d) for details on model formulation.

compartment whose concentration determines the rate at which the cell divides. Note that, because all parameters in Eq. (6c) also appear in one of the other equations, it is possible to calibrate the model using only observations of phytoplankton population size and external nitrate and ammonium concentrations, and to infer changes in internal N from the fitted parameter values (De La Rocha et al., 2010; Malerba et al., 2012). Specifically, these fitted parameters determine the concentration of internal N at which cell division stops (Q_{min}) and the initial quota concentrations at the start of each experiment (Q_{init}). For experiments in which cells were experimentally starved, Q_{init} was set at Q_{min}.

Overall, there are some physiological differences between nitrate and ammonium assimilation in phytoplankton cells that our model had to simplify in order to allow calibration from observations of only medium N and population size. For instance, assimilated ammonium can only be stored as organic N (mainly amino acids or N-containing pigments), and therefore its assimilation rate is influenced by the carbon availability of the cell (Crawford et al., 2000). Conversely, nitrate can also be stored in its inorganic form, but its assimilation is dependent on photosynthetic electron transport for the production of reduced ferredoxin (Crawford et al., 2000). We experimentally controlled for the influence of carbon limitation by ensuring pH levels below 7, using magnetic stirrers to continuously suspend the cultures, supplying air, and by collecting data at the same time in the diel cycle. Furthermore, high concentrations of ammonium have been shown to become cytotoxic due to formation of un-ionized ammonia from the ammonium ion in response to photosynthesis-induced high culture pH (Kallqvist and Svenson, 2003; Yoshiyama and Sharp, 2006). In this study, ammonium-derived ammonia toxicity was avoided by maintaining culture pH below 7. The absence of ammonium-induced ammonia toxicity was confirmed in a specific experiment (see *N starvation followed by* NH_4^+ *repletion* in Section 2.2.1).

2.2. Experimental design

Monoclonal 1.2 L batch cultures of the ecologically ubiquitous and commercially important green alga *Chlorella* sp. (Kallqvist and Svenson, 2003; Yoshiyama and Sharp, 2006; culture accession NQAIF 305, sourced from the North Queensland Algal Culturing and Identification Facility at James Cook University, Townsville, QLD) were reared in standard Bold Basal Medium (BBM; Nichols, 1973). Nitrogen (N) was set as the limiting factor for growth in all experimental cultures, supplied at 1/8 to 1/4 the recommended BBM concentration either as sodium nitrate ($NaNO_3$) for nitrate-BBM, or ammonium chloride (NH_4Cl) for ammonium-BBM, or both (see specific experiment descriptions below). Furthermore, dissociation of the ammonium ion (NH_4^+) into volatile un-ionised ammonia (NH_3) was minimized by ensuring pH levels below 7 by buffering the modified nitrate-BBM and ammonium-BBM media with *4-(2-hydroxyethyl)-1-piperazineethanesulfonic acid* (HEPES) at 8 mmol L^{-1} and $NaHCO_3$ at 2.38 mmol L^{-1} (Vaddella et al., 2011). Cultures were kept in a temperature-controlled room at 27 ± 3°C with a 14–10 h day–night cycle at a light intensity of 45 μmol photons m^2 s^{-1}. Cultures were continuously mixed with magnetic stirrers at 300 rpm (IKA RCT Basic, IKA Labortechnik, Germany) and aerated with 0.45 μm filtered air (Durapore, Millipore). For all experiments, daily triplicate measurements cell numbers were collected by flowcytometry (Guava, Millipore, Hayward, CA, USA) and of N concentrations with the auto-analyser EasyChem Plus (Systea S.p.A., Anagni, Italy), following the manufacturer's EPA-approved and certified protocols (Systea User Manual, 2011). Glassware was acid-washed (10% HCl) and all culturing materials were autoclaved and handled aseptically in a laminar-flow cabinet (Alternative Environmental Solutions fitted with high-efficiency particulate arresting filter, Australia Standards 4260, National Association of Testing Authorities certified).

Time series were collected from 14 different initial conditions of medium NO_3^- and/or NH_4^+, starvation treatment, and initial population size across five different experiments: data from the first 4 experiments were used to calibrate the model, while those collected in the last experiment were used for model validation (i.e. confronting the parameterized model with a new dataset not used for calibration). Experimental designs and starting conditions used for the different experiments were described below.

2.2.1. Calibration experiments

2.2.1.1. Single nitrogen source utilization. To observe the behavior of the species when reared with either nitrate- or ammonium-BBM, two mother cultures were grown in modified BBM medium with the corresponding nitrogen (N) forms and inoculated at 2.5×10^6 cells mL^{-1} ($n = 3$). Initial N concentration was standardized at 400 μmol N L^{-1} of either NO_3^- or NH_4^+.

2.2.1.2. $NO_3^- + NH_4^+$ utilization. To observe growth and N assimilation response to simultaneous and equally concentrated medium nitrate- and ammonium-N, a single N-replete mother culture was reared in nitrate-BBM and used to inoculate 3 independent replicate cultures. Cultures were inoculated with 4.5×10^6 cells mL^{-1} and N was supplied at 400 μmol $N - NH_4^+$ and 400 μmol $N - NO_3^-$.

2.2.1.3. N starvation followed by NO_3^- repletion. To test for the effect of N starvation length on the performance of the nitrate uptake system, a single mother culture reared in nitrate-BBM was starved for 6, 8, 11, 14, and 17 days; for each starvation period a culture was inoculated with 5×10^6 cells mL^{-1} and 400 μmol $N - NO_3^-$ L^{-1} and monitored until stationary phase.

2.2.1.4. N starvation followed by NH_4^+ repletion. To confirm that starvation only affected nitrate assimilation, but not ammonium assimilation, and that our range of ammonium concentrations did not produce cytotoxic effects (both processes not included in the model), a single mother culture reared in ammonium-BBM was used to inoculate 4 independent cultures at 5×10^6 cells mL^{-1}, with a factorial design of 2 levels of starvation (0 and 17 days), each with 2 levels of initial ammonium concentration (200 and 800 μmol $N - NH_4^+$ L^{-1}). The experiment confirmed that NH_4^+ was assimilated

immediately, irrespective of starvation status, and that rates for the highest population growth did not differ between low and high ammonium concentrations (data not shown).

2.2.2. Validation experiments

2.2.2.1. Ammonium-acclimatization after N starvation. To test whether acclimatizing cells with N resupplied as ammonium could eliminate the starvation effect on initial nitrate assimilation, a single 17-day starved mother culture was used to inoculate 3 independent cultures at an initial density of 5×10^6 cells mL^{-1} and 500 μmol $N - NH_4^+ L^{-1}$. When ammonium was depleted, an additional 1000–1500 μmol $N - NO_3^- L^{-1}$ was supplied to test the response of the same culture under repleted conditions. These trajectories were compared to 2 additional equally inoculated cultures that did not receive ammonium acclimatization but an equal concentration of 500 μmol $N - NO_3^- L^{-1}$.

2.3. Model calibration

We used maximum likelihood methods to fit Eqs. (6a–d) to data from the first four experiments simultaneously. This way, model predictions generated from a single set of parameters were confronted with time series from 12 different combinations of initial nitrate, ammonium, population density, and starvation length. Note that all of the parameters that influence the dynamics of the unobserved state (internal quota, $Q(t)$) also appear in the equations for the dynamics of one of the observed states. Flux into the quota can be inferred from changes to medium nitrate and ammonium, while flux out of the quota can be inferred from changes in population density. Note that this would not be true if we had multiple internal pools *sensu* Flynn and Fasham (1997) or Flynn et al. (1997), with fluxes between them. Indeed, when we explored a model with a glutamine pool between inorganic N uptake and a fully assimilated internal quota, numerical algorithms failed to converge on best-fit parameters because compensatory changes in model parameters involving the flux between the glutamine pool and the internal quota produced equally good fit to the data (results not shown).

Two different sources of error can affect parameter calibration from time-series data: process noise and observation error (Bolker, 2008; Hilborn and Mangel, 1997). Process noise refers to unexplained variation due to natural stochasticity in the culture dynamics, while observation error refers to unexplained variation caused by measurement error. The appropriate way to fit the model and calculate parameter best estimates depends on which type of error dominates in the system. When process noise dominates over observation error, then measurements for the state variables will generally be much closer to the system's true state than the predicted values, so observed states at time t should be used to predict states at time $t+1$. Conversely, when observation error dominates over process error, then model predictions are likely to be closer to the true values of the state variables than the measured values, so predicted states at time t should be used to predict states at time $t+1$.

For highly controlled microbial laboratory systems, observation error is often quite small, and it is reasonable to assume that process noise dominates the random variation in the data (Bolker, 2008). Indeed, in our data, there was strong evidence that this was the case: the standard deviation from the triplicate independent readings offers an independent estimate of the magnitude of the observation error and was usually less than 5% of the total error calculated from model calibration. Consequently, standard one-step ahead techniques were employed to account for process noise during parameter calibration (Bolker, 2008; Hilborn and Mangel, 1997). For our dataset, the function for the negative log-likelihood score ($-L$) assuming normally-distributed process noise is:

$$-L_{t,i}\left\{Y_{t,i} | f\left(Y_{t-1,i}\right), \sigma_i^2\right\} = -\frac{n}{2}\ln(2\pi) - \frac{n}{2}\ln\left(\sigma_i^2\right) - \frac{1}{2\sigma_i^2} \times \left(Y_{t,i} - f\left(Y_{t-1,i}\right)\right)^2 \quad (7)$$

where i indexes each state variable (i.e. nitrate, ammonium, and population density), t indicates time (days since the start of the experiment), n is the length of the time series, σ_i^2 is the variance of state variable i, and $Y_{t,i}$ and $f(Y_{t-1,i})$ are the observed value of state variable i at time t, and the corresponding model predicted value (calculated from Eqs. (6a–d) based on the observed state at time $t-1$), respectively. Maximum likelihood parameter estimates were obtained by minimizing Eq. (7) summed across all t, all i, and all calibration experiments using the unconstrained general-purpose optimization function nlminb() in the software program R (R Core Team, 2014).

2.4. Model selection

To assess how the parameterization of individual functional responses contributed to the model fit, we compared the fit of the fully parameterized model against reduced versions, where particular functional responses were simplified or excluded. We used Akaike's Information Criterion (AIC) to select the best fitting model. The best model was the one that minimized the formula $-2 \times L + 2 \times k$, where L is the log-likelihood score and k is the total number of calibrated parameters (Bozdogan, 1987). The model with the lowest AIC is the estimated best model. In general, models within 2 AIC units of the best model should be considered as having significant statistical support (Burnham and Anderson, 2002). We also confirmed that alternative model selection techniques of Bayesian Information Criterion (BIC) and Likelihood Ratio Testing produced the same conclusions as AIC. For the best model, we calculated 95% profile likelihood confidence intervals for each of the estimated parameters and we evaluated the model's goodness of fit by inspecting how evenly the residuals were distributed across replicate cultures for each day of the different experiments.

2.5. Model validation

While experiments including different degrees of starvation or simultaneous exposure to nitrate and ammonium include unique information about the behavior of the species, single N utilization and acclimatization experiments include information also present in at least one other experiment. Time-series from the acclimatization experiment (see Section 2.2.2.1) represent the most novel and challenging set of initial conditions. Therefore, the data from this experiment were excluded from model calibration and were instead used for model validation: after using data from the first 4 experiments to select the best model, and to estimate the maximum likelihood parameter estimates for that model, the same parameter values were used to predict the trajectories of the 5 other independent cultures inoculated with 17-day starved cells, re-supplied with either ammonium ($n=3$) or nitrate ($n=2$), and finally supplied with a pulse of new nitrate. To quantify the fit, a standard coefficient of determination $\left(R^2_{\text{pred}}\right)$ between the model prediction and the observed values for each state variable of each experiment was calculated as follows:

$$R^2_{\text{pred}} = 1 - \frac{\sum_{c=1}^{n}\sum_{d=1}^{7}\left(y_{c,d} - \hat{y}_{c,d}\right)^2}{\sum_{c=1}^{n}\sum_{d=1}^{7}\left(y_{c,d} - \bar{y}_c\right)^2} \quad (8)$$

where c indexes the independent cultures, d indexes the observations for each day within each culture, $y_{c,d}$ is the observed value from culture c at day d, $\hat{y}_{c,d}$ is the corresponding predicted value

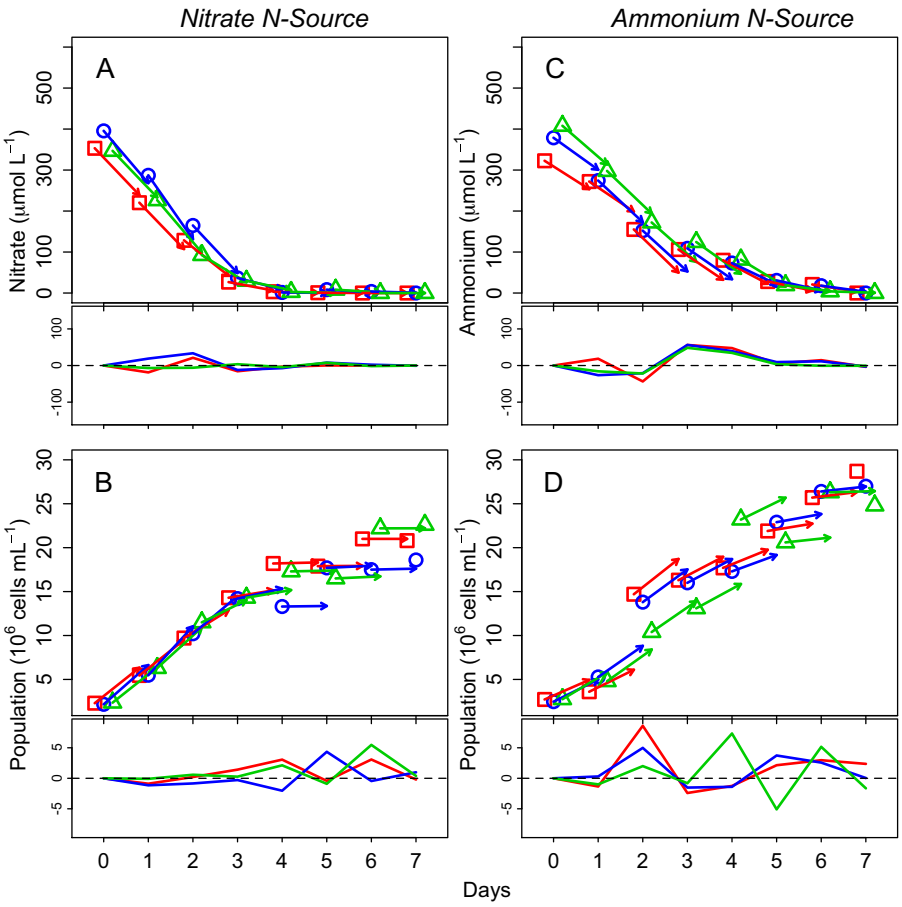

Fig. 2. Time-series for medium nitrogen (A and C) and population size (B and D) for *Chlorella* sp. reared in batch culture with either nitrate (A and B) or ammonium (C and D) as the only nitrogen sources. Each symbol type is an independent replicate culture and each point is the mean between three replicate measurements for that culture. Arrows show one-step ahead predictions for the best-fit model assuming process noise, where the observed values at time t (base of arrows) are used in Eqs. (6a–d) to predict values at time $t+1$ (arrowheads; see Section 2.2.1). Line graphs beneath each panel connect the residuals between model predictions and observations for each day and are a different color for each different replicate culture. Vertical axes are scaled consistently across the two sub-panels. (For interpretation of the references to color in this figure legend, the reader is referred to the web version of this article.)

generated by the calibrated model with Eqs. (6a–d), and $\bar{y}_c$ is the mean value from culture c across the time-series (Lindstrom et al., 1999; Turchin, 1996). To further evaluate the predictive ability of the model, we also report the R^2_{pred} coefficients from the only other possible cross-validation configuration, where the *single nitrogen source utilization* experiments were used as validating datasets, and all other data were used as training datasets.

3. Results

3.1. Model calibration and model selection

The model described the data for our first four experiments reasonably well (Figs. 2–4). Model selections with AIC and BIC both indicated that observations of *Chlorella* sp. were best described by a model assuming linear nitrate and ammonium assimilation and incorporating nitrate starvation and ammonium-induced nitrate uptake inhibition (Table 2). Alternative model selection technique of Likelihood Ratio Testing produced identical conclusions (results not shown). Maximum likelihood estimates and 95% confidence limits were successfully identified for all model parameters, and they indicate that *Chlorella* sp. exhibited a higher per-cell uptake rate for nitrate over ammonium (compare w_{NO_3} and w_{NH_4} in Table 1).

The first experiments with nitrate- and ammonium-only tested the model against data from two single-N experiments, and showed that, in the absence of starvation or multiple N sources, observed trajectories are well characterized by the model: residual variation was small compared to the mean and symmetrically distributed around zero (Fig. 2), except during days 3 and 4 for the ammonium cultures, where ammonium uptake rates were consistently lower than those predicted by the model. This is apparent in Fig. 2C by arrowheads (model predictions) pointing consistently below observed values at days 3 and 4, yielding positive residuals across all replicates for those days. The second experiment tested the model against time-series of *Chlorella* sp. reared with nitrate and ammonium simultaneously, which the model also captured reasonably well (Fig. 3). This included up to an approximately one-day delay in nitrate uptake due to fast rates of ammonium uptake, followed by a return to rapid nitrate uptake by the second day (initial horizontal trajectories, followed by rapid declines in Fig. 3A). There was a time delay between N assimilation and population growth that the model did not capture: the rapid increase in population density resulting from the substantial $NO_3^- + NH_4^+$ uptake at day 2 was predicted to take place at day 3, but was mainly observed at days 4 and 5. This is apparent by arrowheads pointing above the observed values (all negative residuals) at day 3, while pointing consistently below the observed values (all positive residuals) at days 4 and 5 (Fig. 3C). However, the overall good fit indicates that the model was able to simultaneously (i.e., with the same fitted parameters) explain both nitrate- and ammonium-only growth, as well as growth with the two nutrients in equal quantities, with relatively small errors in the timing of when the most rapid changes occurred.

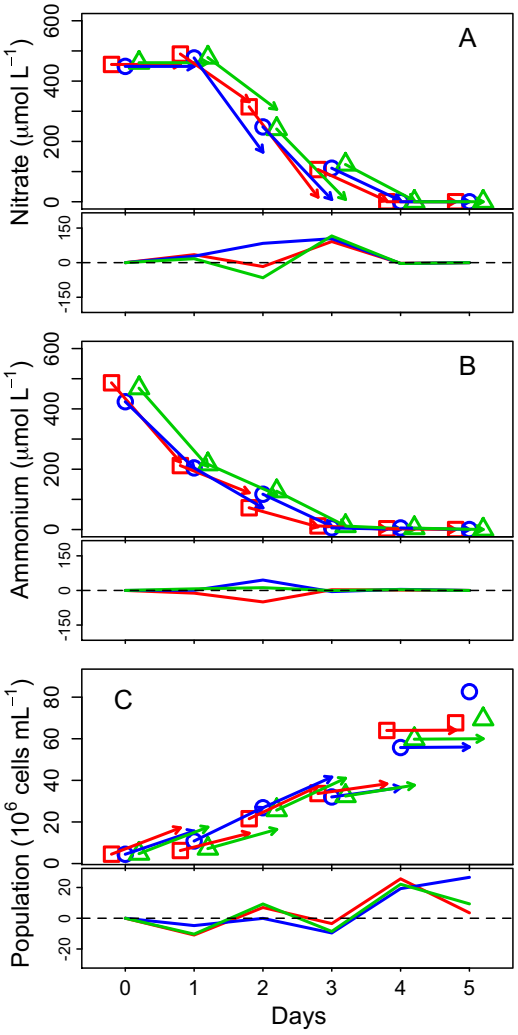

Fig. 3. Time-series and model fit for medium nitrate (A), medium ammonium (B), and population size (C) for *Chlorella* sp. reared in the presence of both forms of nitrogen. Each symbol type is an independent replicate culture and each point is the mean between three replicate measurements for that culture. Arrows (top panel) and lines (bottom panel) show the predicted values for the best-fit model and its residuals. See Fig. 2 legend for further details.

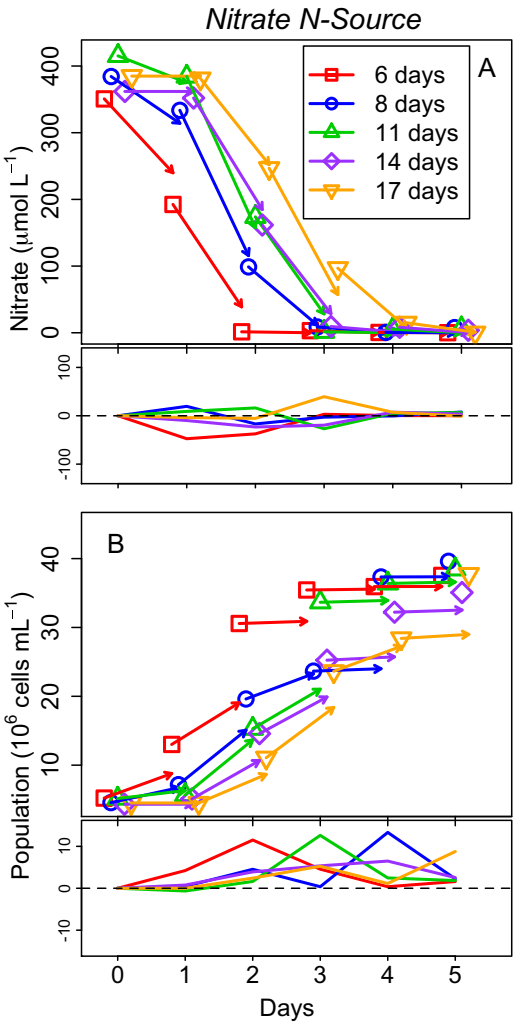

Fig. 4. Time-series and model fit for medium nitrate (A) and population size (B) of a nitrogen-starved inoculum of *Chlorella* sp. resupplied with nitrate. Legend indicates the length (days) of starvation imposed before starting the experiment. Each point represents the mean between three replicate measurements for each culture. Arrows (top panel) and lines (bottom panel) show the predicted values for the best-fit model and its residuals. See Fig. 2 legend for further details.

N starvation had an important effect on nitrate uptake in *Chlorella* sp. (Fig. 4A and B). Model selection favored a functional response in which activation of the nitrate uptake system is delayed by a brief (<1 day) period that is proportional to the length of starvation experienced before the experiment (Table 2), which the model captured well across all starvation treatments (residuals approximately evenly spread among negative and positive values in Fig. 4A). Data on population growth for N-starved cultures resupplied with nitrate showed evidence of temporal correlation in the residuals. Population size trajectories were under-predicted by the model, with arrowheads consistently pointing below observed values (mostly positive residuals in Fig. 4B). This indicates that cells displayed greater efficiency in converting N into new cells than the model could capture. Starvation only affected nitrate uptake, as ammonium assimilation did not show any delays, even after 17 days of starvation (data not shown).

3.2. Model validation

Using parameter estimates from fits of the previous four experiments, data from acclimatization experiments (see Section 2.2.2.1) were used to test the predictive power of the model. R^2_{pred} coefficients were generally very high (0.86–0.99; Fig. 5). Acclimatizing 17-day starved cultures with a preliminary pulse of ammonium removed any initial delay in nitrate assimilation (no nitrate uptake delay after day 5 in Fig. 5B). Conversely, acclimatizing equivalently starved cells with nitrate showed an initial 24-h delay in nitrate uptake and cell division that is consistent with nitrate starvation experiments (cf. horizontal orange arrows at day 0 for 17-day starved treatment in Fig. 4A with two horizontal arrows at day 0 in Fig. 5E). Once cells recovered from starvation, the rate of per-cell nitrate assimilation did not differ between nitrate- and ammonium-acclimatized cultures (comparable uptake at day 5 between Fig. 5B and E). The only lack of fit occurred between days 1 and 3, where the model predicted a slower rate of ammonium depletion (arrows pointing consistently above observed values, yielding negative residuals for these days in Fig. 5C) than occurred in the cultures. Finally, the excellent prediction ability of the model was further confirmed by repeating cross-validation using the *single nitrogen utilization experiments* as validating datasets and all other experiments as training datasets: R^2_{pred} for all state variables were between 0.85 and 0.99, very similar to the R^2_{pred} values reported in our original validation experiment (Fig. 5). Because

Table 2
Formal model selection with Akaike Information Criterion (AIC) and Bayesian Information Criterion (BIC) between functional responses for nitrate and ammonium uptake (f_N), rehabilitation time following nitrogen starvation (r_N), and ammonium-induced inhibition on nitrate uptake (I_{inh}). We compared the fit of the full model against reduced versions, where particular functional responses were simplified or excluded from the fully parameterized model. Biological interpretation and scores for maximum negative log-likelihood ($-L$), AIC, difference in AIC (ΔAIC), BIC, difference in BIC (ΔBIC) are reported between competing models for each functional response (FR), with their corresponding number of calibrated parameters in brackets (no. of pars). Boldface indicates the estimated best-fitting model and therefore the one employed for parameter estimation. See Eqs. (2a,b)–(5) for full functional responses, Section 2.4, and Table 1 for parameter definitions, units, and calibrated values.

FR	Competing models for each FR [no. of pars]		Nitrate ($N = NO_3$)					Ammonium ($N = NH_4$)					Biological
			$-L$	AIC	ΔAIC	BIC	ΔBIC	$-L$	AIC	ΔAIC	BIC	ΔBIC	Interpretation
f_N	(1)	$w_N \times N(t)$ [23]	**−3068**	**6182**	**0**	**6277**	**0**	**−3068**	**6182**	**0**	**6277**	**0**	Functional response for the uptake of a single cell (1) Increases linearly with N
	(2)	v_N [23]	−3156	6358	176	6453	176	−3189	6424	242	6519	242	(2) Fix for any N
	(3)	$v_N \times \left(N(t)/(N(t)+k_N)\right)$ [24]	−3068	6184	2	6283	6	−3068	6184	2	6283	6	(3) Saturates at high N
r_{NO_3}	(1)	$\begin{cases} 0 & \text{if } t_{st} < d_{NO_3} \\ c_{NO_3} \times \left(t_{st} - d_{NO_3}\right) & \text{otherwise} \end{cases}$ [24]	−3068	6184	2	6283	6						Starvation-induced delay on nitrate uptake (1) Linearly proportional to starvation length after d_N days of starvation
	(2)	$\begin{cases} 0 & \text{if } t_{st} < d_{NO_3} \\ c_{NO_3} \times t_{st} & \text{otherwise} \end{cases}$ [23]	**−3068**	**6182**	**0**	**6277**	**0**						(2) Linearly proportional to starvation length
	(3)	0 [22]	−3133	6310	128	6401	124						(3) No starvation effect
I_{inh}	(1)	$I_{inh}(NH_4(t)) = \begin{cases} 1 & \text{if } f_{NH_4}(NH_4(t)) < f_{NH_4\_crit} \\ 0 & \text{otherwise} \end{cases}$ [24]						**−3068**	**6184**	**0**	**6283**	**0**	Ammonium-induced inhibition on nitrate uptake (1) Threshold at $f_{NH_4\_crit}$
	(2)	1 [23]						−3093	6232	48	6327	44	(2) No Inhibition

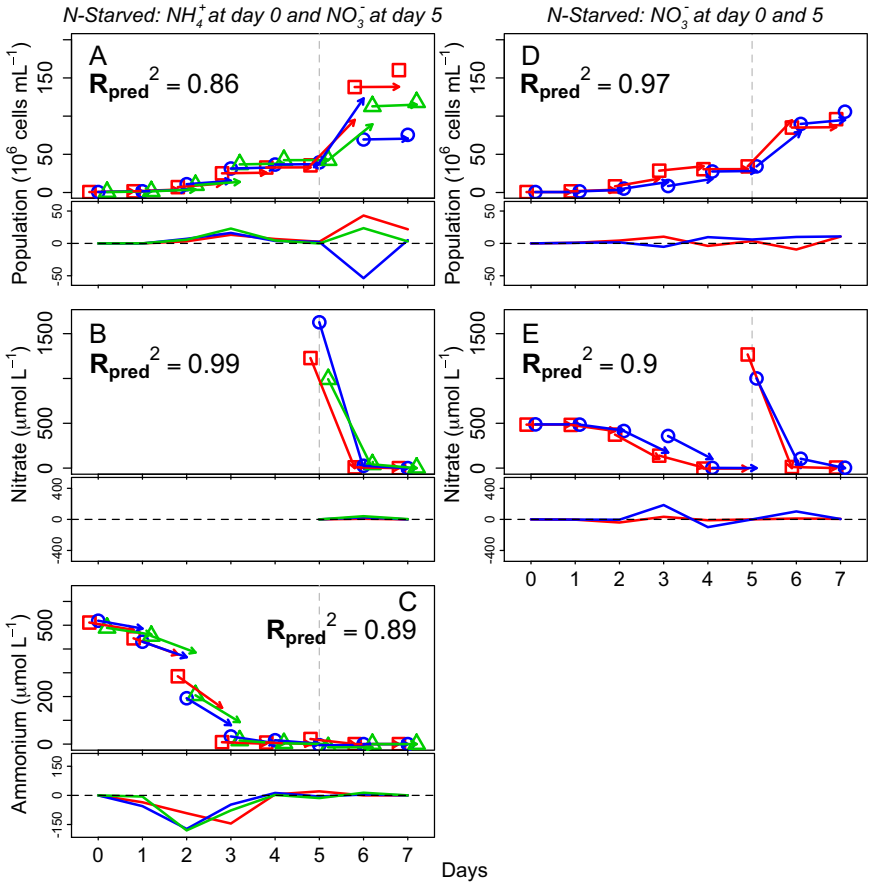

Fig. 5. Model validation with time-series from a 17-day starved inoculum of *Chlorella* sp. not included during model calibration. Left column—time-series for population size (A) resupplied at day 0 with ammonium (B) and at day 5 with nitrate (gray dashed vertical line in (C)). Right column—time-series for population size (D) resupplied with nitrate (E) both at day 0 and at day 5. Each symbol type is an independent replicate culture and each point is the mean between three replicate measurements for that culture. Arrows (top panel) and lines (bottom panel) show the predicted values for the best-fit model and its residuals. See Fig. 2 legend for further details.

fitted and predicted trajectories in this second exercise were virtually identical to those shown in Figs. 2–5, we have not reproduced them here.

4. Discussion

Our results show that a single set of model parameters can characterize well the coupled dynamics between nitrate and ammonium uptake and cell division in the green algal species *Chlorella* sp. reared in batch culture under a wide range of initial conditions. Analyzing nitrate–ammonium utilization with the present model allowed us to quantify functional responses for assimilation of nitrate and ammonium individually or combined, as well as effects of nitrogen (N) starvation or ammonium-induced nitrate uptake inhibition on nitrate uptake. Furthermore, high R^2_{pred} scores recorded during model validation suggest that the model describes culture trajectories well even under novel experimental conditions.

While previous studies have quantified assimilation responses to a few particular starvation lengths, the present study is the first to calibrate a functional response quantifying delay in nitrate uptake as a continuous function of starvation length. The physiological reason for such delay is a slow recovery in nitrate-reductase activity following N starvation, which acts as the limiting step for nitrate assimilation and amino acid incorporation into proteins (Dortch et al., 1982). This explanation is also consistent with our observed absence in a delay for ammonium uptake following starvation, as no enzymatic reduction is required for its assimilation (Crawford et al., 2000). Proteins involved in the reduction of nitrate to organic N were recorded to decrease by in abundance by 60–90% in the diatom *Thalassiosira pseudonana* at the onset of N starvation (Hockin et al., 2012). Different species display variable delay times to starvation: 1 and >2.5 h delays for 3 and 4 days of starvation (Martinez, 1991) and 2 h for 3 days of starvation for the diatom *Skeletonema costatum* (Dortch et al., 1982), 8 h for 3 days of starvation for the dinoflagellate *Amphidinium carterae* (Dortch et al., 1982), and no delay for the green alga *Dunaliela tetriolecta* (Dortch et al., 1982). These observed delay times are comparable with presently calibrated functional responses for *Chlorella* sp., where 3 and 4 days of starvation would correspond to 5 and 7 h of delay, respectively. In nature, some species, mostly diatoms, form fortnightly algal blooms near estuaries correlated with tidal cycles (Parsons et al., 1983; Zamon, 2002). One potential explanation is that, within phytoplankton communities, some species are adapted to respond quickly to nutrient fluxes after extended starvation periods (Largier, 1993). This hypothesis could be tested by calibrating and comparing the shapes of the functional responses for the recovery rate of nitrate uptake to N starvation $\left(r_{NO_3}\right)$ for species that commonly produce algal blooms, and those that do not.

Interestingly, the effect of starvation on nitrate assimilation was removed when starved cultures were first acclimated with ammonium before supplying nitrate (Fig. 5). This result is consistent with earlier work on *Chlorella vulgaris*, where the production of nitrate reductase, a specific enzyme required for nitrate assimilation, increased when cells were reared in ammonium following N starvation (Morris and Syrett, 1965). Also the marine haptophyte *Isocrysis galbana* registered a low but constant production of nitrate reductase when reared with ammonium as the only N source (Flynn

et al., 1993). In contrast, synthesis of nitrate reductase did not occur in cells of the freshwater rhodophyte *Cyanidium caldarium* grown in ammonium-based media (Rigano and Violante, 1973). The lack of a clear trend across species poses further complications in our understanding of the general role of nitrate and ammonium fluctuations in the regulation of phytoplankton communities.

Analyzing episodes in which the model failed to reproduce observed trajectories can indicate mis-specification of functional forms or implicate biological responses not explicitly incorporated in the model. For instance, discrepancies between the data and our model indicated that the rate at which assimilated N was converted into new cells was more rapid in cultures recovering from N starvation compared to replete conditions (mostly positive residuals in Fig. 4B). A possible explanation is that cells with insufficient N for production of new biomass will channel excess carbon produced from photosynthesis into storage molecules such as triglyceride or starch (Zhang et al., 2013). This produces an increase in the C:N ratio that can enhance growth rate following N resupply (Bittar et al., 2013). *Chlorella* sp. has been documented to display a significant increase in lipid and carbohydrate contents in response to N starvation conditions (Zhang et al., 2013). Thus, one area for refinement for our model would be to explicitly account for the relationship between N starvation, carbon content of a cell, and per-cell rate of population growth.

Despite decades of research, the role of different N sources on the ecology of autotrophic communities remains unclear (Boudsocq et al., 2012; Schimel and Bennett, 2004). For phytoplankton, this problem has implications for a broad range of aquatic systems: from coastal areas, where seasonal precipitation or tidal regimes drive large fluctuations in N availability at multiple scales, to inland basins, experiencing temporally variable anthropologic N release from fertilizers or waste-water discharge (Domingues et al., 2011). The present data on nitrate and ammonium assimilation clearly show that there are major differences in how cells take up and assimilate these two different N sources. The modeling approach presented and tested here can contribute to our understanding of how different N supplies influence growth and interactions of phytoplankton communities in nature.

Acknowledgments

This research was supported by AIMS@JCU (www.aims.jcu.edu.au), the Australian Institute of Marine Science (www.aims.gov.au), and James Cook University (www.jcu.edu.au). This research contributes to the MBD Energy Research and Development program for Microalgal Carbon Capture and Storage supported by the Advanced Manufacturing Cooperative Research Centre, funded through the Australian Government's Cooperative Research Centre Scheme.

We are grateful to the North Queensland Algal Identification and Culturing Facility. In particular, we thank Stan Hudson and Florian Berner for their support in laboratory procedures. We also thank the Ecological Modelling Research Group at James Cook University, especially Shane Blowes for comments on earlier drafts of the work. Finally, thanks to Dr Christopher Klausmeier and Dr Elena Litchman at the Kellogg Biological Station for helpful advice and constructive criticism.

References

Berges, J.A., 1997. Minireview: algal nitrate reductases. Eur. J. Phycol. 32, 3–8.
Bittar, T.B., Lin, Y.J., Sassano, L.R., Wheeler, B.J., Brown, S.L., Cochlan, W.P., Johnson, Z.I., 2013. Carbon allocation under light and nitrogen resource gradients in two model marine phytoplankton. J. Phycol. 49, 523–535.
Bolker, B., 2008. Dynamic models. In: Bolker, B. (Ed.), Ecological Models and Data in R. Princeton University Press, Princeton, NJ (pp. vii, 396).
Boudsocq, S., Niboyet, A., Lata, J.C., Raynaud, X., Loeuille, N., Mathieu, J., Blouin, M., Abbadie, L., Barot, S., 2012. Plant preference for ammonium versus nitrate: a neglected determinant of ecosystem functioning? Am. Nat. 180, 60–69.
Bozdogan, H., 1987. Model selection and Akaike Information Criterion (AIC)—the general-theory and its analytical extensions. Psychometrika 52, 345–370.
Bronk, D.A., See, J.H., Bradley, P., Killberg, L., 2007. DON as a source of bioavailable nitrogen for phytoplankton. Biogeosciences 4, 283–296.
Burnham, K.P., Anderson, D.R., 2002. Model Selection and Multimodel Inference: A Practical Information-Theoretic Approach, second ed. Springer-Verlag, New York, NY.
Collos, Y., Gagne, C., Laabir, M., Vaquer, A., Cecchi, P., Souchu, P., 2004. Nitrogenous nutrition of *Alexandrium catenella* (Dinophyceae) in cultures and in Thau lagoon, southern France. J. Phycol. 40, 96–103.
Cox, T.J.S., Maris, T., Soetaert, K., Conley, D.J., Van Damme, S., Meire, P., Middelburg, J.J., Vos, M., Struyf, E., 2009. A macro-tidal freshwater ecosystem recovering from hypereutrophication: the Schelde case study. Biogeosciences 6, 2935–2948.
Crawford, N.M., Kahn, M.L., Leustek, T., Long, S.R., 2000. Nitrogen and sulfur. In: Buchanan, B.B., Gruissem, W., Jones, R.L. (Eds.), Biochemistry & Molecular Biology of Plants. American Society of Plant Physiologists, Rockville, MD, pp. 786–849 [Great Britain].
Cullimore, J.V., Sims, A.P., 1981. Glutamine-synthetase of *Chlamydomonas*—its role in the control of nitrate assimilation. Planta 153, 18–24.
De La Rocha, C.L., Terbruggen, A., Volker, C., Hohn, S., 2010. Response to and recovery from nitrogen and silicon starvation in *Thalassiosira weissflogii*: growth rates, nutrient uptake and C, Si and N content per cell. Mar. Ecol. Prog. Ser. 412, 57–68.
Domingues, R.B., Barbosa, A.B., Sommer, U., Galvao, H.M., 2011. Ammonium, nitrate and phytoplankton interactions in a freshwater tidal estuarine zone: potential effects of cultural eutrophication. Aquat. Sci. 73, 331–343.
Donald, D.B., Bogard, M.J., Finlay, K., Leavitt, P.R., 2011. Comparative effects of urea, ammonium, and nitrate on phytoplankton abundance, community composition, and toxicity in hypereutrophic freshwaters. Limnol. Oceanogr. 56, 2161–2175.
Dortch, Q., 1990. The interaction between ammonium and nitrate uptake in phytoplankton. Mar. Ecol. Prog. Ser. 61, 183–201.
Dortch, Q., Clayton, J.R., Thoreson, S.S., Bressler, S.L., Ahmed, S.I., 1982. Response of marine-phytoplankton to nitrogen deficiency—decreased nitrate uptake vs enhanced ammonium uptake. Mar. Biol. 70, 13–19.
Droop, M.R., 1975. Nutrient status of algal cells in batch culture. J. Mar. Biol. Assoc. U.K. 55, 541–555.
Duarte, C.M., Cebrià n, J., 1996. The fate of marine autotrophic production. Limnol. Oceanogr. 41, 1758–1766.
Dugdale, R.C., Wilkerson, F.P., Hogue, V.E., Marchi, A., 2007. The role of ammonium and nitrate in spring bloom development in San Francisco Bay. Estuarine Coast. Shelf Sci. 73, 17–29.
Fan, C., Glibert, P.M., Alexander, J., Lomas, M.W., 2003. Characterization of urease activity in three marine phytoplankton species, *Aureococcus anophagefferens*, *Prorocentrum minimum*, and *Thalassiosira weissflogii*. Mar. Biol. 142, 949–958.
Flynn, K.J., Fasham, M.J.R., 1997. A short version of the ammonium–nitrate interaction model. J. Plankton Res. 19, 1881–1897.
Flynn, K.J., Zapata, M., Garrido, J.L., Opik, H., Hipkin, C.R., 1993. Changes in carbon and nitrogen physiology during ammonium and nitrate nutrition and nitrogen starvation in *Isochrysis galbana*. Eur. J. Phycol. 28, 47–52.
Flynn, K.J., Fasham, M.J.R., Hipkin, C.R., 1997. Modelling the interactions between ammonium and nitrate uptake in marine phytoplankton. Philos. Trans. R. Soc., Ser. B: Biol. Sci. 352, 1625–1645.
Fowler, D., Coyle, M., Skiba, U., Sutton, M.A., Cape, J.N., Reis, S., Sheppard, L.J., Jenkins, A., Grizzetti, B., Galloway, J.N., Vitousek, P., Leach, A., Bouwman, A.F., Butterbach-Bahl, K., Dentener, F., Stevenson, D., Amann, M., Voss, M., 2013. The global nitrogen cycle in the twenty-first century. Philos. Trans. R. Soc., Ser. B—Biol. Sci. 368.
Griffiths, M.J., van Hille, R.P., Harrison, S.T., 2014. The effect of nitrogen limitation on lipid productivity and cell composition in *Chlorella vulgaris*. Appl. Microbiol. Biotechnol. 98, 2345–2356.
Gruber, N., 2008. The marine nitrogen cycle: overview and challanges. In: Capone, D.G., Bronk, D.A., Mulholland, M.R., Carpenter, E.J. (Eds.), Nitrogen in Marine Environement. , second ed. Elsevier, Amsterdam.
Guerrero, M.G., Vega, J.M., Losada, M., 1981. The assimilatory nitrate-reducing system and its regulation. Annu. Rev. Plant Physiol. Plant Mol. Biol. 32, 169–204.
Hilborn, R., Mangel, M., 1997. The Ecological Detective: Confronting Models with Data. Princeton University Press, Princeton, NJ; Chichester, pp. 131–171.
Hockin, N.L., Mock, T., Mulholland, F., Kopriva, S., Malin, G., 2012. The response of diatom central carbon metabolism to nitrogen starvation is different from that of green algae and higher plants. Plant Physiol. 158, 299–312.
Jackson, L.E., Schimel, J.P., Firestone, M.K., 1989. Short-term partitioning of ammonium and nitrate between plants and microbes in an annual grassland. Soil Biol. Biochem. 21, 409–415.
Kallqvist, T., Svenson, A., 2003. Assessment of ammonia toxicity in tests with the microalga, *Nephroselmis pyriformis*, Chlorophyta. Water Res. 37, 477–484.
Largier, J.L., 1993. Estuarine fronts—how important are they. Estuaries 16, 1–11.
Laws, E.A., Pei, S.F., Bienfang, P., Grant, S., 2011. Phosphate-limited growth and uptake kinetics of the marine prasinophyte *Tetraselmis suecica* (Kylin) Butcher. Aquaculture 322, 117–121.
Legovic, T., Cruzado, A., 1997. A model of phytoplankton growth on multiple nutrients based on the Michaelis–Menten–Monod uptake, Droop's growth and Liebig's law. Ecol. Model. 99, 19–31.
L'Helguen, S., Maguer, J.-F., Caradec, J., 2008. Inhibition kinetics of nitrate uptake by ammonium in size-fractionated oceanic phytoplankton communities: implications for new production and F-ratio estimates. J. Plankton Res. 30, 1179–1188.
Lindstrom, J., Kokko, H., Ranta, E., Linden, H., 1999. Density dependence and the response surface methodology. Oikos 85, 40–52.

Lomas, M.W., 2004. Nitrate reductase and urease enzyme activity in the marine diatom *Thalassiosira weissflogii* (Bacillariophyceae): interactions among nitrogen substrates. Mar. Biol. 144, 37–44.

Maguer, J.F., L'Helguen, S., Madec, C., Labry, C., Le Corre, P., 2007. Nitrogen uptake and assimilation kinetics in *Alexandrium minutum* (Dynophyceae): effect of N-limited growth rate on nitrate and ammonium interactions. J. Phycol. 43, 295–303.

Malerba, M.E., Connolly, S.R., Heimann, K., 2012. Nitrate–nitrite dynamics and phytoplankton growth: formulation and experimental evaluation of a dynamic model. Limnol. Oceanogr. 57, 1555–1571.

Martinez, R., 1991. Transient nitrate uptake and assimilation in *Skeletonema costatum* cultures subject to nitrate starvation under low irradiance. J. Plankton Res. 13, 499–512.

Michalczyk, A., Kersebaum, K., Roelcke, M., Hartmann, T., Yue, S.C., Chen, X.P., Zhang, F.S., 2014. Model-based optimisation of nitrogen and water management for wheat-maize systems in the North China Plain. Nutr. Cycl. Agroecosyst. 98, 203–222.

Morris, I., Syrett, P.J., 1963. The development of nitrate reductase in *Chlorella* and its repression by ammonium. Arch. Mikrobiol. 47, 32–41.

Morris, I., Syrett, P.J., 1965. The effect of nitrogen starvation on the activity of nitrate reductase and other enzymes in *Chlorella*. J. Gen. Microbiol. 38, 21–28.

Mulholland, M.R., Lomas, M.W., 2008. Nitrogen uptake and assimilation. In: Capone, D.G., Bronk, D.A., Mulholland, M.R., Carpenter, E.J. (Eds.), Nitrogen in Marine Environement. , second ed. Elsevier, Amsterdam, pp. 303–384.

Nichols, H.W., 1973. Growth media—freshwater. In: Stein, J. (Ed.), Handbook of Phycological Methods. Cambridge University Press, Cambridge, p. 448.

Parker, R.A., 1993. Dynamic-models for ammonium inhibition of nitrate uptake by phytoplankton. Ecol. Modell. 66, 113–120.

Parsons, T.R., Perry, R.I., Nutbrown, E.D., Hsieh, W., Lalli, C.M., 1983. Frontal zone analysis at the mouth of Saanich Inlet, British-Columbia, Canada. Mar. Biol. 73, 1–5.

Pistorius, E.K., Funkhouser, E.A., Voss, H., 1978. Effect of ammonium and ferricyanide on nitrate utilization by *Chlorella vulgaris*. Planta 141, 279–282.

Priddle, J., Whitehouse, M.J., Atkinson, A., Brierley, A.S., Murphy, E.J., 1997. Diurnal changes in near-surface ammonium concentration—interplay between zooplankton and phytoplankton. J. Plankton Res. 19, 1305–1330.

R Core Team, 2014. R: A Language and Environment for Statistical Computing. R Foundation for Statistical Computing, Vienna, Austria, ⟨http://www.R-project.org/⟩.

Rigano, C., Violante, U., 1973. Effect of nitrate, ammonia and nitrogen starvation on regulation of nitrate reductase in *Cyanidium caldarium*. Arch. Mikrobiol. 90, 27–33.

Rigano, C., Dimartinorigano, V., Vona, V., Fuggi, A., 1979. Glutamine-synthetase activity, ammonia assimilation and control of nitrate reduction in the unicellular red alga *Cyanidium caldarium*. Arch. Microbiol. 121, 117–120.

Schimel, J.P., Bennett, J., 2004. Nitrogen mineralization: challenges of a changing paradigm. Ecology 85, 591–602.

Syrett, P.J., 1981. Nitrogen metabolism of microalgae. Can. Bull. Fish. Aquat. Sci. 210, 182–210.

Syrett, P.J., Morris, I., 1963. The inhibition of nitrate assimilation by ammonium in *Chlorella*. Biochim. Biophys. 67, 566–575.

Tantanasarit, C., Englande, A.J., Babel, S., 2013. Nitrogen, phosphorus and silicon uptake kinetics by marine diatom *Chaetoceros calcitrans* under high nutrient concentrations. J. Exp. Mar. Biol. Ecol. 446, 67–75.

Thacker, A., Syrett, P.J., 1972. Assimilation of nitrate and ammonium by *Chlamydomonas reinhardi*. New Phytol. 71, 423-&.

Turchin, P., 1996. Nonlinear time-series modeling of vole population fluctuations. Res. Popul. Ecol. 38, 121–132.

Vaddella, V.K., Ndegwa, P.M., Jiang, A., 2011. An empirical model of ammonium ion dissociation in liquid dairy manure. Trans. ASABE 54, 1119–1126.

Varela, D.E., Harrison, P.J., 1999. Effect of ammonium on nitrate utilization by *Emiliania huxleyi*, a coccolithophore from the oceanic northeastern Pacific. Mar. Ecol. Prog. Ser. 186, 67–74.

Yoshiyama, K., Sharp, J.H., 2006. Phytoplankton response to nutrient enrichment in an urbanized estuary: apparent inhibition of primary production by overeutrophication. Limnol. Oceanogr. 51, 424–434.

Young, E.B., Beardall, J., 2003. Photosynthetic function in *Dunaliella tertiolecta* (Chlorophyta) during a nitrogen starvation and recovery cycle. J. Phycol. 39, 897–905.

Zamon, J.E., 2002. Tidal changes in copepod abundance and maintenance of a summer Coscinodiscus bloom in the southern San Juan Channel, San Juan Islands, USA. Mar. Ecol. Prog. Ser. 226, 193–210.

Zehr, J.P., Ward, B.B., 2002. Nitrogen cycling in the ocean: new perspectives on processes and paradigms. Appl. Environ. Microbiol. 68, 1015–1024.

Zhang, Y.M., Chen, H., He, C.L., Wang, Q., 2013. Nitrogen starvation induced oxidative stress in an oil-producing green alga *Chlorella sorokiniana* C3. PLoS ONE 8, e69225.